

# Uvitron's Optical Research Program Report

Goran Arbanas

©2003 Uvitron International, Inc.  
380 Union St., West Springfield, MA 01089  
[www.uvitron.com](http://www.uvitron.com)

March 13, 2003

## **Abstract**

We present a theoretical framework and a corresponding computer model for design and optimization of reflective mirrors used in Uvitron's UV light products. Our computer model enables Uvitron to design mirrors to generate a desired UV output, optimized for a particular UV curing application.

Our model takes into account a spatial distribution of light intensity inside a UV lamp, which is a key ingredient needed to make our model's prediction agree with experimental results.

We derive mathematical expressions used in our model. We assume cylindrical symmetry of our system, whereby reducing our system to two dimensions. We describe how we arrived to an accurate expression for spatial distribution of light radiation within a mercury vapor lamp. We present our numerical findings.

# Contents

<b>1</b>	<b>Introduction</b>	<b>3</b>
1.1	Motivation . . . . .	3
1.2	Inception Uvitron’s Optical Research Program (ORP) . . . . .	4
1.3	Outline of this Report . . . . .	4
1.4	Reflected Light Outshines Direct Light . . . . .	5
<b>2</b>	<b>Result Summary</b>	<b>6</b>
2.1	Polar Coordinates . . . . .	7
2.2	Cartesian Coordinates . . . . .	8
2.3	Distributed Light Source . . . . .	10
<b>3</b>	<b>Geometric Derivation of Results</b>	<b>12</b>
3.1	Arrival Position of Reflected Ray . . . . .	12
3.2	Direct Light Irradiation Intensity . . . . .	15
3.3	Point Source Translation . . . . .	16
<b>4</b>	<b>Numerical Method</b>	<b>21</b>
4.1	Implementation in Math Modeling Software . . . . .	21
4.2	Sample Output . . . . .	22
4.3	Time-Relaxation Method . . . . .	22
4.4	Conclusions . . . . .	23

# Chapter 1

## Introduction

### 1.1 Motivation

Uvitron's products are used in a variety of manufacturing and other settings to provide UV light optimized for a given application. Some applications of UV light require a narrow beam of UV light for small curing areas, others may require a wider beam, and yet others may require an exotic intensity distribution needed for a specialized use.

Such a wide variety of requirements can now be met without costly and time consuming prototype building, thanks to the optical model presented here. This model allows Uvitron to modularize its product line by designing products in which several types of mirrors could be employed, depending on the product application.

Our model can be used in two different ways:

- To compute UV intensity distribution for a given reflective mirror of an arbitrary shape
- To compute optimal mirror shape which generates a required UV intensity distribution

Each mode of usage listed above allows for a spatially distributed lamp to be employed in computation. The size of the lamp is parametrized in our model allowing us to see the effects of a various lamps available on the UV market.

## 1.2 Inception Uvitron's Optical Research Program (ORP)

Being well aware that the UV light intensity output is the ultimate measure of Uvitron products' success, Uvitron's Engineering has initiated Optical Research Program (ORP) to complement its already renown expertise in solid-state power supply design. The synergy between the Uvitron's ORP and the solid-state design expertise gives Uvitron a strategically advantageous position to increase its lead as a price/performance leader in the field of UV light manufacturers.

The mission of the ORP was to develop a complete array of tools to analyze, model, and design the most efficient optical equipment for a given product and its application. The ORP effort is sub-divided into three categories:

- Development of foundation in geometry and physics
- Implementation of theoretical results into computer simulation model
- Experimental validation of model output

Our research into optimization of optical parameters proved that by varying the parameters of the reflector shape, as well as those of the light source itself, it is possible to devise an optimal light intensity output for a given application. Uvitron has successfully leveraged ORP's research result, with implemented improvements across its line of products.

Even though most of the UV light products on the market consist of a single light source and a reflector, the industry as a whole hasn't invested much effort on optimization of the reflectors optical.

We revisit the most common mirror shapes encountered in the industry, such as conic sections, in order to analyze the effect of spatially distributed light sources, such as cylindrically symmetric pressurized Hg vapor lamp, and other variables.

## 1.3 Outline of this Report

In Chapter 2 we summarize theoretical results, which are derived in greater detail in Chapter 3.

In Chapter 4 we outline technical aspects of computer model implementation

## 1.4 Reflected Light Outshines Direct Light

To a very good approximation, we assume that our entire system, comprised of a point light source, a reflector of an arbitrary shape, and the exposed flat surface, possesses a cylindrical symmetry, i.e. is independent of the z-axis, leaving us with 2-dimensional system to analyze.

The total irradiation received at the flat surface consists of the light reflected by the mirror,  $I_r$ , and the light directly imparted by the light source onto the surface,  $I_d$ . At the first sight, it would seem that the direct component would be stronger than the reflected component, but this preconception is easily dispelled by considering a mirror in the shape of parabola with a point source in its focus.

The intensity of light reflected from an ideal parabolic mirror is independent of the distance from the mirror, when a point light source is placed in parabola's focus. The reflected light intensity,  $I_r$ , is inversely proportional to the parabola's focal length,  $I_r \sim 1/f$ , and is independent of distance  $D$  between the point light source and the irradiated surface.

$I_r$  is much greater than the intensity of direct irradiation,  $I_d$ , which is inversely proportional to the distance  $D$  between the light source and the irradiated surface,  $I_d \sim 1/D$ . Thus for a sufficiently large distance  $D$ , the direct irradiation component can be deemed practically negligible, and for distances involved with Uvitron's product, i.e.  $D \approx 5''$ , we find it to be only 10% of the total light output, the remaining 90% coming from the reflector.

A common example of this effect is a household flashlight which produces a strong beam of light thanks to its parabolic mirror. In fact, a simple flashlight proved to be a confidence boosting test case for our model, as we could compare theory vs. experiment simply by shining a flashlight onto a flat surface in a dark room and observing the light patterns as we tweaked the flashlight's "focus".

## Chapter 2

# Result Summary

In this chapter we present equations for the spatial intensity of light output reflected<sup>1</sup> from a mirror of an arbitrary shape onto a flat surface. (We will derive the analogous expression for direct light in Chapter 3.)

We introduce a simplifying approximation by imposing cylindrical symmetry, thus reducing a three-dimensional problem to a two-dimensional, planar, system. We do this in two systems of planar coordinates:

- Polar coordinates  $(r, \theta)$
- Cartesian coordinates  $(x, y)$

The advantage of polar coordinates is that it is straightforward to account for *rotation* of the reflector, by substituting  $(r, \theta) \rightarrow (r, \theta - \theta_0)$  where  $\theta_0$  is the angle of rotation.

The advantage of Cartesian coordinate system is that it makes it convenient to account for *translation* of the reflector by substituting  $(x, y) \rightarrow (x - x_0, y - y_0)$

Our model allows for reflector shapes to be defined in either polar or Cartesian coordinates. In either case we place the origin of the coordinate system at a point from which the expressions for the mirror are simple. In case of conic sections in polar coordinates, for example, the origin of a coordinate system is usually placed at the conic's focal point, but it could be any other point, at the expense of introducing algebraic complexity.

Conic sections (circle, ellipse, parabola, and hyperbola) have been used for reflector shapes because of their optical properties related to their construction about focal point(s).

---

<sup>1</sup>In this report we consider only a single reflection, although our formalism lends itself for use with multiple reflections.

Conic sections in polar coordinates can be expressed as:

$$m(\theta) = \frac{s}{1 + e \cdot \cos \theta} \quad (2.1)$$

where  $s = m(\theta = \pi/2)$  is the *semi-latus rectum*, while  $e$  denotes a curve's eccentricity. Eccentricity has the following values for conic sections:

conic section	value of $e$
circle	0
ellipse	$0 < e < 1$
parabola	1
hyperbola	$1 < e$

Polar coordinates representation of conic sections can be cast into Cartesian coordinates equivalents via the following transformations (here the conic section has its focus at  $(x, y) = (0, 0)$ , is symmetric about the  $y$ -axis<sup>2</sup>, and is facing downwards):

$$r \rightarrow \sqrt{x^2 + y^2} \quad (2.2)$$

$$\cos \theta \rightarrow \frac{y}{\sqrt{x^2 + y^2}} \quad (2.3)$$

which upon substitution yields:

$$(1 - e^2)y^2 + x^2 + 2esy = s^2 \quad (2.4)$$

Although conic sections will be used frequently throughout this report, the following treatise applies to any well behaving curve  $m(\theta)$ .

## 2.1 Polar Coordinates

We present the final expressions for the spatial intensity of the reflected light  $I_r$ <sup>(3)</sup> in a parametric form where polar angle  $\theta$  is a parameter and  $X(\theta)$  is the distance between the point of arrival of the reflected light ray on the illuminated surface and the point on the same surface immediately below the center of the light source:

<sup>2</sup>If we used  $x$ -axis for  $\theta = 0$  we would simply exchange  $x$  and  $y$  coordinates to obtain more common, but equivalent, expressions

<sup>3</sup>subscript  $r$  in  $I_r$  indicates reflected light intensity as opposed to its direct counterpart  $I_d$ , where the total intensity  $I = I_r + I_d$ . In most cases encountered in practice  $I_r \gg I_d$  further demonstrating the importance of reflecting mirror design!

$$I_r(X) = \begin{pmatrix} I_r(\theta) \\ X(\theta) \end{pmatrix} \quad (2.5)$$

where

$$I_r(\theta) \sim \frac{d\theta}{dX(\theta)} = \left( \frac{dX(\theta)}{d\theta} \right)^{-1} \quad (2.6)$$

and

$$X(\theta) = \frac{m(\theta) - D \cdot (\Gamma_- \sin \theta - \cos \theta)}{\Gamma_- \cos \theta + \sin \theta} \quad (2.7)$$

where for convenience we define  $\Gamma_{\pm}$  as:

$$\Gamma_{\pm} = \frac{m^2 \pm m'^2}{2 m m'} \quad (2.8)$$

$$= \frac{1}{2} \left( \frac{m}{m'} \pm \frac{m'}{m} \right) \quad (2.9)$$

and  $m = m(\theta)$  is the equation of the reflector in polar coordinates,  $m' = \frac{dm(\theta)}{d\theta}$ .

Making the above substitutions one obtains:

$$I_r(\theta) \sim \frac{\Gamma_- \cos \theta + \sin \theta}{[m' + m\Gamma_-][\Gamma_- \cos \theta + \sin \theta] - \Gamma_+^2 [1 + 2 \frac{m'^2 - m''}{m^2 + m'^2}][D + m \cos \theta]} \quad (2.10)$$

Note that  $I_r(\theta)$  for parabola is independent of distance  $D$  because  $1 + 2 \frac{m'^2 - m''}{m^2 + m'^2} = 0$  for a parabola given by  $m(\theta) = s/(1 + \cos \theta)$ .

## 2.2 Cartesian Coordinates

We present a spatial intensity distribution of the reflected light  $I_r$  as a function of distance  $x$ , in a parametric form:

$$I_r(X) = \begin{pmatrix} I_r(x) \\ X(x) \end{pmatrix} \quad (2.11)$$

$$I_r(x) \sim \frac{d\theta(x)}{dX(x)} = \frac{\frac{d}{dx} \theta(x)}{\frac{d}{dx} X(x)} \quad (2.12)$$

We simply reuse the equation for  $X(\theta)$  in Eq. (2.7) by expressing  $\theta$  as a function of  $x$  and  $y(x)$  everywhere on the r.h.s of that equation as follows:

$$X(x) = \frac{m(\theta(x)) - D[\Gamma_- \sin \theta(x) - \cos \theta(x)]}{\Gamma_- \cos \theta(x) + \sin \theta(x)} \quad (2.13)$$

$$\Gamma_- = \frac{m(x)^2 - m'(x)^2}{2m(x)m'(x)} \quad (2.14)$$

$$m'(x) = \frac{dm(x)}{d\theta(x)} = \frac{\frac{d}{dx}m(x)}{\frac{d}{dx}\theta(x)} \quad (2.15)$$

$$m(x) = \sqrt{x^2 + y(x)^2} \quad (2.16)$$

$$\theta(x) = \arctan\left(-\frac{x}{y(x)}\right) \in [-\pi, \pi] \quad (2.17)$$

The expression for  $\theta(x)$  above takes into account our choice of  $\theta = 0$  along positive  $y$ -axis, with  $\theta$  counter-clockwise. It is important that the arctan function returns value between  $-\pi$  and  $\pi$  to get the correct physical angle with respect to  $\theta = 0$ <sup>4</sup>

A downward facing parabola of a focal length  $s/2$  and the center of the Cartesian coordinate system  $(x, y) = (0, 0)$  at parabola's focal point gives for  $y(x)$  (see eq. (2.4)):

$$y(x) = -\frac{1}{2s}x^2 + \frac{s}{2} \quad (2.18)$$

To translate  $y(x)$  by  $x_0$  in the  $x$ -direction and  $y_0$  in the  $y$  direction simple make the following substitution.

$$y(t) \rightarrow y(t - x_0) + y_0 \quad (2.19)$$

One also has to make the substitution

$$D \rightarrow D - y_0 \quad (2.20)$$

to correct for the change in the distance between the point source and the exposed surface. For rotation in polar coordinates,  $D$  remains unchanged.

---

<sup>4</sup>In numerical implementation, this requirement meant invoking a hybrid implementation of arctan function, e.g. ATAN2 in MathCAD.

## 2.3 Distributed Light Source

To create a realistic model of a light source we derived an equation for the spatial distribution of light output intensity of a cylindrically symmetric light source. A sample lamp we used to develop and validate our model was a cylindrically symmetric pressurized mercury lamp of .5" diameter, with its highest intensity output at its center, tapering off towards its walls.

To determine the light output of our cylindrical lamp, we utilized the following two graphs from [1]:

- Plasma's relative temperature  $T/T_{r=0}$  as a function of relative distance  $r/R$  from the center of the cylinder. (Figure 6.6 of [1])
- Semi log plot of radiation from mercury as a function of inverse temperature  $1/T$

Based on the above two diagrams one can express a relative radiation (i.e. light output) as a function of (relative) radial distance, by algebraic elimination of temperature, as:

$$\mu(r/R) = e^{-\frac{\alpha}{1-(r/R)^2}} \quad (2.21)$$

where  $\alpha = 0.67$  gives a good agreement with the graphs above, as well as the measured experimental data we collected in the process of developing our model.

It is worthwhile to emphasize here that our model only gives a relative distribution of the light output, as our primary goal was to find the mirror that would generate a desired relative distribution of light output. Adjusting for a particular normalization amounts to an overall multiplication by a constant factor, which does not affect the substance of our model in its present application.

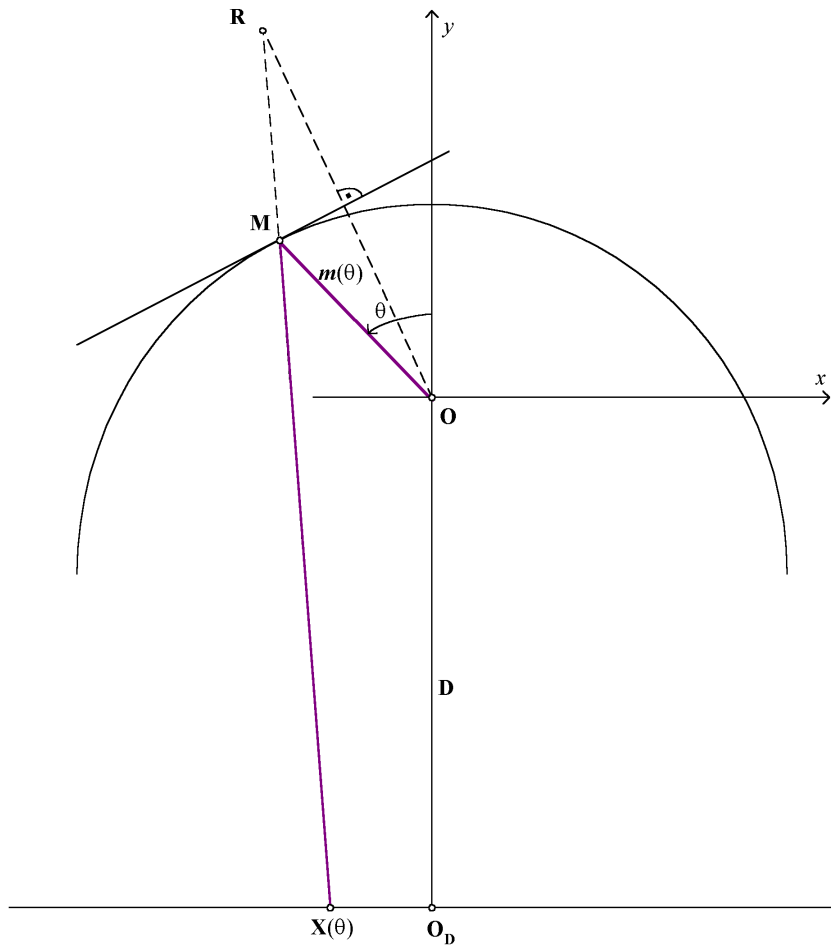


Figure 2.1: This diagram show a path of a light ray emitted from its source at origin  $O$ , reflected from the mirror at point  $M$ , and imparted onto a horizontal surface at point  $X(\theta)$ . Point  $R$  is the mirror image of  $O$  with respect to a tangent through point  $M$ . Point  $R$  is where the reflected source appears to be to the observer at  $X(\theta)$ . Mirror is defined by a radial function  $m(\theta)$ , but it could be expressed in any coordinate system; we shall derive equivalent expressions in Cartesian coordinates. We only consider a single light ray reflection, to minimize the loss of intensity incurred by multiple mirror reflections. Fortunately, this requirement simplifies the algebra involved in this analysis.

## Chapter 3

# Geometric Derivation of Results

In this chapter we derive the result that were summarized in Chapter 2. The reader is advised to consult Figures [3.1], [3.2], [3.3], at the end of this Chapter, where all of the quantities used in this derivation are displayed graphically.

### 3.1 Arrival Position of Reflected Ray

In this section we derive an expression for the position at which the reflected ray arrives to the cured surface, as a function of the ray's emission angle  $\theta$ . We use  $X(\theta)$  to denote the distance between the position of arrival and  $O_D$  (see Fig. [3.1]). The intensity of reflected light at  $X(\theta)$  is then  $I_r = \frac{d\theta}{dX(\theta)}$ .

We start out by writing an expression for  $X(\theta, \alpha)$  where  $\alpha$  is the angle of the mirror tangent at the reflection point  $M$  (see Fig. [3.1]). We then eliminate  $\alpha$  in terms of  $\theta$  to get  $X(\theta)$ .

Tangent angle  $\alpha$  in Fig. 3.1 is:

$$\tan \alpha = \frac{dy(x)}{dx} = \frac{\frac{dm_y(\theta)}{d\theta}}{\frac{dm_x(\theta)}{d\theta}} = \frac{\frac{d(m(\theta) \cos \theta)}{d\theta}}{\frac{d(-m(\theta) \sin \theta)}{d\theta}} = \frac{m'(\theta) \cos \theta - m(\theta) \sin \theta}{-m'(\theta) \sin \theta - m(\theta) \cos \theta} \quad (3.1)$$

The minus sign in  $m_x(\theta) = -m(\theta) \sin \theta$  is due to our choice to align  $\theta = 0$  with positive  $y$ -axis and a counter-clockwise rotation of  $\theta$ .

It is convenient to find the  $x$  and  $y$  coordinates of the light source mirror image  $R$  with respect to the tangent at the reflection point  $M$ . We label the Cartesian coordinates of the reflected light source as  $(R_x, R_y)$ :

$$(R_x, R_y) = 2m(\theta) \cos(\theta - \alpha) \cdot (\sin \alpha, \cos \alpha) \quad (3.2)$$

and use these to express the position of ray's arrival at the flat irradiated surface,  $X(\theta, \alpha)$ , as a function of the emission angle  $\theta$  and the tangent angle  $\alpha$  defined above (see Fig. [3.1]):

$$X(\theta, \alpha) = R_x - d \cdot \sin \gamma \quad (3.3)$$

where

$$d = \frac{R_y + D}{\cos \gamma}; \quad \gamma = 2\alpha - \theta \quad (3.4)$$

Substituting (2.4) and (2.5) into (2.3) yields:

$$X(\theta, \alpha) = \frac{m(\theta) \sin(2\alpha - 2\theta) - D \sin(2\alpha - \theta)}{\cos(2\alpha - \theta)} \quad (3.5)$$

In the above expression for  $X(\theta, \alpha)$ , we need to eliminate  $\alpha$  in favor of  $\theta$ , in order to obtain  $x(\theta, \alpha)$  as a function of ray's emission angle  $\theta$  alone. Elimination of  $\alpha$  in favor of  $\theta$  at this stage is greatly simplifies the derivation of reflected light intensity  $I_r$  as  $I_r \sim \frac{d\theta}{dX}$ . First we derive expressions for  $\sin(\alpha)$  and  $\cos(\alpha)$  consistent with the expression for  $\tan \alpha$  in (3.1), and normalized as

$$\sin^2 \alpha + \cos^2 \alpha = 1:$$

$$\sin \alpha = \frac{m'(\theta) \cos \theta - m(\theta) \sin \theta}{\sqrt{m(\theta)^2 + m'(\theta)^2}} \quad (3.6)$$

$$\cos \alpha = \frac{-m'(\theta) \sin \theta - m(\theta) \cos \theta}{\sqrt{m(\theta)^2 + m'(\theta)^2}} \quad (3.7)$$

It is useful to derive expressions for  $\sin(2\alpha)$  and  $\cos(2\alpha)$ , as the expression for  $X(\theta, \alpha)$  is a function of  $(2\alpha)$  alone. Here we use basic trigonometric equalities  $\sin(2\alpha) = 2 \sin \alpha \cos \alpha$  and  $\cos(2\alpha) = \cos^2 \alpha - \sin^2 \alpha$ , and the equations (3.6) and (3.7):

$$\sin(2\alpha) = \frac{1}{\Gamma_+(\theta)} [\Gamma_- \sin(2\theta) - \cos(2\theta)] \quad (3.8)$$

$$\cos(2\alpha) = \frac{1}{\Gamma_+(\theta)} [\Gamma_- \cos(2\theta) + \sin(2\theta)] \quad (3.9)$$

where  $\Gamma_{\pm}$  are auxiliary, dimensionless functions:

$$\Gamma_{\pm} = \frac{m(\theta)^2 \pm m'(\theta)^2}{2m(\theta)m'(\theta)} \quad (3.10)$$

and  $m'(\theta) = \frac{dm(\theta)}{d\theta}$ .

Eliminating  $\alpha$  in favor of  $\theta$  and  $m(x)$  we get:

$$X(\theta) = \frac{m(\theta) - D \cdot (\Gamma_-(\theta) \sin \theta - \cos \theta)}{\Gamma_-(\theta) \cos \theta - \sin \theta} \quad (3.11)$$

Having found the expression for  $X(\theta)$  we express the light intensity  $I_r(\theta)$  received at  $X(\theta)$  as a differential of emission angle  $d\theta$  per distance  $dX(\theta)$  (see Fig. [3.2]):

$$I_r(\theta) \sim \frac{d\theta}{dX(\theta)} = \left( \frac{dX(\theta)}{d\theta} \right)^{-1} \quad (3.12)$$

The above expression for  $I_r(\theta)$  has a simple physical interpretation as the density of light rays  $d\theta$  imparted to  $dX(\theta)$ . The greater density of imparted light rays, arriving at  $X(0)$ , the greater the irradiation. An underlying assumption here is that the point source emits light equally in all directions. Furthermore, since we are only interested in a relative irradiation, we are not concerned with absolute values of  $I_r$ . The absolute value amounts to determining a normalization constant, call it  $N$ , such that  $N \int (I_r + I_d) dX = P$  where  $P$  is the lamp's Power expressed in Watts.

The expressions for  $X(\theta)$  and  $I_r(\theta)$  provide a parametric definition of  $I_r(X)$  with  $\theta$  acting as a parameter:

$$I_r(X) \sim \left( \begin{array}{c} I_r(\theta) \\ X(\theta) \end{array} \right) \quad (3.13)$$

For the sake of completeness we write down the expression for  $I_r(\theta)$ .

$$I_r(\theta) \sim \frac{\Gamma_- \cos \theta + \sin \theta}{[m' + m\Gamma_-][\Gamma_- \cos \theta + \sin \theta] - \Gamma_+^2 [1 + 2 \frac{m'^2 - m''}{m^2 + m'^2}][D + m \cos \theta]} \quad (3.14)$$

Note that  $I_r(\theta)$  for parabola is independent of distance  $D$  because  $1 + 2 \frac{m'^2 - m''}{m^2 + m'^2} = 0$  for a parabola  $m(\theta) = s/(1 + \cos \theta)$  as expected, since the rays reflected by a parabola are parallel to the axis of symmetry.

In addition to verifying the validity of our formalism with parabolic mirror, we verified it with a planar mirror  $m(\theta) \sim \cos^{-1} \theta$  and a circular mirror<sup>1</sup>  $m(\theta) = 1$ , since exact solutions can be found by simpler methods which utilize the symmetries of these two cases, and the results of our formalism have been confirmed in these cases.

### 3.2 Direct Light Irradiation Intensity

Irradiation density of direct light emission will be expressed as a function of distance  $I_d(X)$ , and then transformed into a parametric form with emission angle  $\theta$  as a parameter in the same fashion as  $I_r$  in Eq. (3.12). With parametric form of  $I_d$ , we can then add it to parametric form of  $I_r$  to get a total radiation intensity at  $X(\theta)$ .

$$\cos \theta = \frac{D}{\sqrt{X^2 + D^2}} \quad (3.15)$$

Our goal is to obtain  $I_d(X) \sim \left(\frac{d\theta}{dX}\right)$  by differentiating both sides of the above equation with respect to  $X$ :

$$-\sin \theta \cdot \frac{d\theta}{dX} = \left(-\frac{1}{2}\right) \frac{2D \cdot X}{(X^2 + D^2)^{3/2}} \quad (3.16)$$

and substituting

$$\sin \theta = \frac{X}{\sqrt{X^2 + D^2}} \quad (3.17)$$

we obtain

$$I_d(X) \sim \frac{d\theta}{dX} = \frac{D}{D^2 + X^2} \quad (3.18)$$

where  $D$  is the closest distance between the point source and the flat irradiated surface. In order to be able to correspond the reflected and the direct rays arriving to the same location  $X$ , we convert  $I_d(X)$  into a parametric form by substituting  $X(\theta)$  for  $X$ :

$$I_d(X) = \left( \begin{array}{c} I_d(\theta) \\ X(\theta) \end{array} \right) \quad (3.19)$$

where

---

<sup>1</sup>For circle we need use Eq. (2.7) to get  $X(\theta) = -D \tan(\theta)$

$$I_d(\theta) \sim \frac{d\theta}{dX} = \frac{D}{D^2 + X(\theta)^2} \quad (3.20)$$

and

$$X(\theta) = \frac{m(\theta) - D \cdot (\Gamma_-(\theta) \sin \theta - \cos \theta)}{\Gamma_-(\theta) \cos \theta - \sin \theta} \quad (3.21)$$

So that the total irradiation density is simply the sum of the  $I_r$  and  $I_d$ :

$$I_t(X) = \begin{pmatrix} I_r(\theta) + I_d(\theta) \\ X(\theta) \end{pmatrix} \quad (3.22)$$

### 3.3 Point Source Translation

In this subsection we calculate the irradiation of a point source translated by a distance  $T$  from the origin of the coordinate system  $O$ , at an angle  $\beta$  counter-clockwise from the vertical axis. We shall utilize this result to determine irradiation from a distributed light source, since a distributed source can be approximated as a spatial distribution of suitably attenuated point sources. For our purposes we assume the each point source remains isotropic, although its intensity is attenuated to conserve normalization and to account for variation of intensity due to points location within a lamp (see Section 2.3).

The polar angle in the coordinate system of the translated source,  $\phi$ , can be expressed as a function of  $T$ ,  $\beta$ , and  $m(\beta)$  of the untranslated coordinate system where the expression for  $m(\beta)$  is known. An expression for  $m(\theta)$  is not necessarily known in the translated coordinate system, in which case the following derivation is required.

$$\tan \phi(\theta) = \frac{m(\theta) \sin \theta - T \sin \beta}{m(\theta) \cos \theta - T \cos \beta} \quad (3.23)$$

The application of cosine theorem yields the following expression.

$$m_T(\theta) = \sqrt{m(\theta)^2 + T^2 - 2Tm(\theta) \cos(\theta - \beta)} \quad (3.24)$$

We have inserted subscript  $T$  in  $m_T(\beta)$  to indicate that the origin has been translated by distance  $T$  at an angle  $\beta$ .

We can now repeat the formalism from the Section 4.1, which gives us an expression for  $X_T(\beta)$  similar in form to  $X(\beta)$ :

$$X_T(\theta) = \frac{m_T(\theta) - D_T \cdot (\Gamma_T(\theta) \sin \phi(\theta) - \cos \phi(\theta))}{\Gamma_T(\theta) \cos \phi(\theta) - \sin \phi(\theta)} \quad (3.25)$$

where the new equation elements are:

$$\Gamma_T = \frac{m_T(\theta)^2 - m'_T(\theta)^2}{2m_T(\theta)m'_T(\theta)} \quad (3.26)$$

$$m'_T(\theta) = \frac{dm_T(\theta)}{d\phi} = \frac{dm_T(\theta)}{d\theta} \left( \frac{d\phi(\theta)}{d\theta} \right)^{-1} \quad (3.27)$$

and  $D_T$  is the distance between the point source in the new coordinate system and the flat irradiated surface:

$$D_T = D + T \cos \beta \quad (3.28)$$

To obtain irradiation density we need to perform a parametric differentiation, as follows:

$$I_T(\theta) = \left( \frac{dX_T(\theta)}{d\phi} \right)^{-1} = \left( \frac{dX_T(\theta)}{d\theta} \right)^{-1} \left( \frac{d\phi(\theta)}{d\theta} \right) \quad (3.29)$$

which together with the expression for  $x_T(\theta)$  allows us to plot  $I_T$  parametrically with  $\theta$  acting as a parameter.



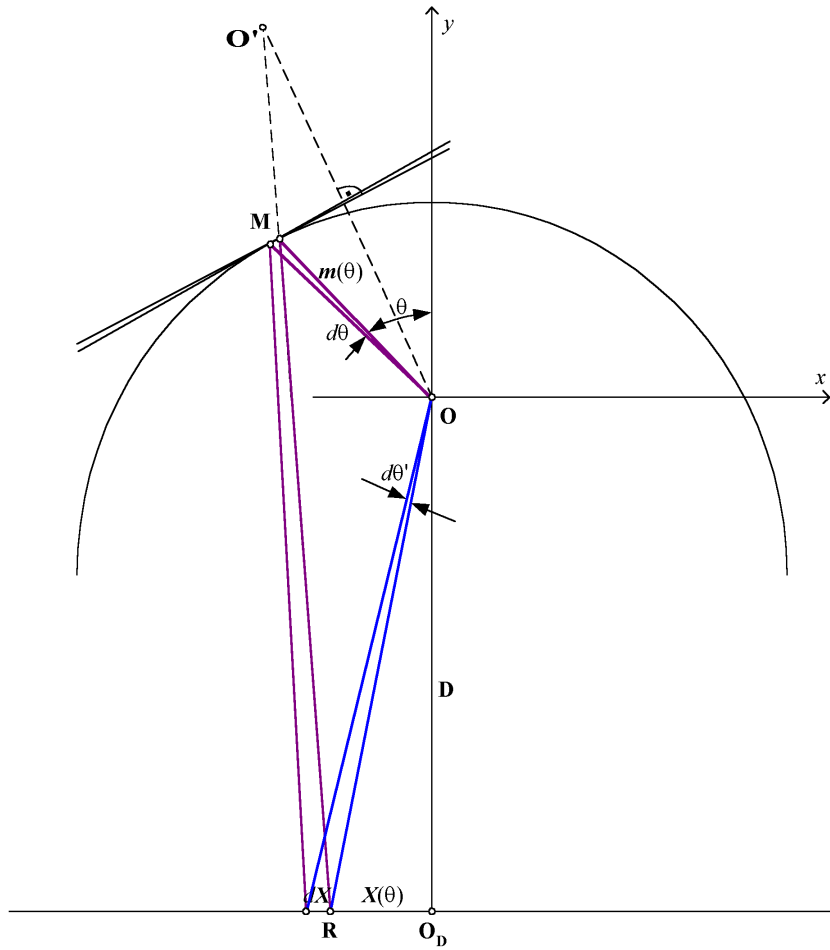


Figure 3.2: Physical interpretation of the expression for irradiation intensity  $I_r(\theta) \sim \frac{d\theta}{dX(\theta)}$ . We assume isotropic source, i.e. source intensity is independent of  $\theta$ , and therefore proportional to  $d\theta$ .

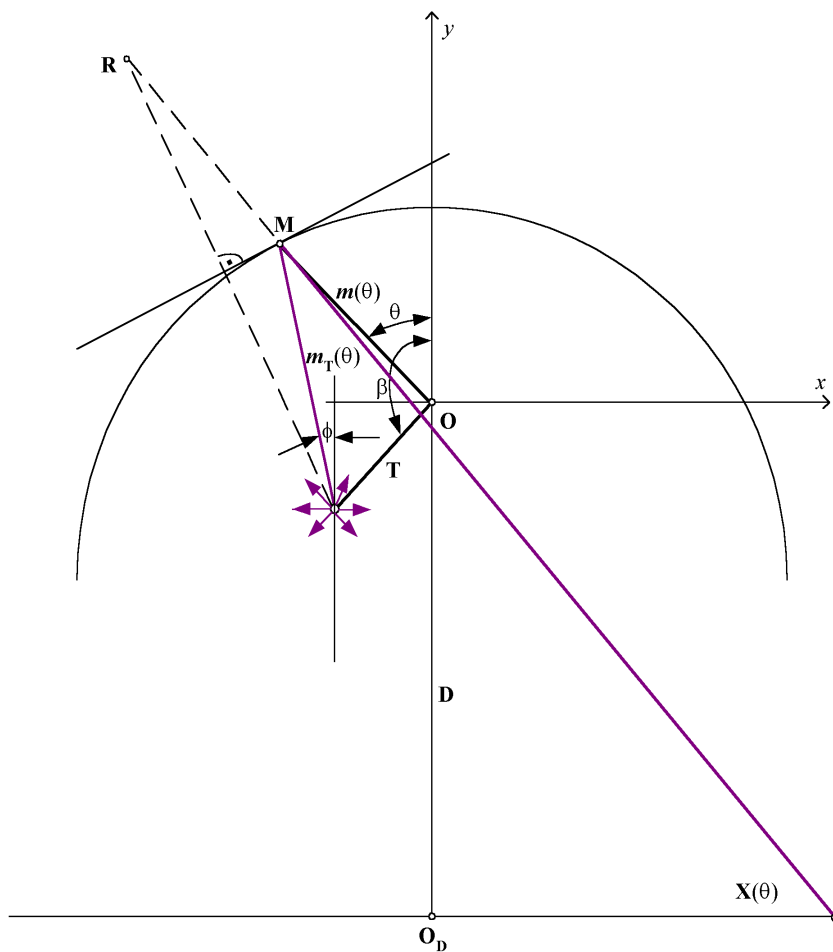


Figure 3.3: This diagram show a path of a (UV) light ray emitted from a translated point  $T O$ , reflected from the mirror at point  $M$ , and imparted onto a horizontal surface at point  $X(\theta)$ . Point  $R$  is the mirror image of  $T$  with respect to a tangent through point  $M$ . Angle  $\beta$  of translation is indicated.

## Chapter 4

# Numerical Method

We employed our theoretical formalism of Chapters 2 and 3 to vary the shape of the mirror, as well as the UV light source, to find a configuration that generates a desired shape of light intensity.

Depending on application of UV curing process, the UV lamp may need to provide distinct UV intensity outputs. Some UV applications require highly focused UV light beams, the others may require that a larger area be illuminated by uniform UV light.

### 4.1 Implementation in Math Modeling Software

We put our distributed light source onto a rectangular  $x$ - $y$  grid, where each grid point served as a *point* light source, as our formalism applies to *point* sources. For a cylindrically symmetric light source, we had to take into account the attenuation of light intensity away from the center of the lamp, as described in Section 2.3 and given by Eq. (2.21). Note that for the point light sources on this grid we need to use the formalism for a translated point source, Eq. (3.25), as these points are not in focus.

For each grid point source we had several hundred of rays being emitted symmetrically in all directions. For rays hitting the reflector we used Eq. (2.7) for polar coordinates, or Eq. (2.13) for Cartesian coordinates.

We divided the illuminated surface into an arbitrary number of buckets along the  $x$ -axis, and counted how many rays end up in each of the buckets. Plotting the count of rays vs. the distance gives us a non-normalized shape of UV intensity distribution.

## 4.2 Sample Output

We show the results of our model, obtained on MathSoft's MathCAD, for a parabolic mirror of 0.5-inch focal length and an Hg pressurized vapor bulb of 0.3 inches radius, centered at the parabola's focus. The bulb was approximated by 200-point light sources, each point producing 100 light rays. The illuminated surface was approximated by 100 buckets covering an area of 6 inches.

Due to typesetting complications we present the diagrams in a separate file.

## 4.3 Time-Relaxation Method

In this section we present an algorithm for determining the shape of the mirror,  $m(\theta)$ , when only a desired form of light intensity  $I_0(X)$  output is given. For this purpose we present a time-relaxation method, based on minimization of a positive definite quantity, in this case a standard deviation  $\sigma$ :

$$\sigma = \int (I(X) - I_0(X))^2 dX \quad (4.1)$$

where for convenience we normalize  $I(X) > 0$  and  $I_0(X) > 0$ :

$$\int I(X) dX = \int I_0(X) dX = 1 \quad (4.2)$$

Time relaxation method then gives

$$\dot{m}(\theta) = -\frac{\delta\sigma}{\delta m(\theta)} \quad (4.3)$$

Replacing  $\dot{m}(\theta)$  by  $\frac{\Delta m(\theta)}{\Delta t}$  where  $\Delta t$  is a suitably chosen <sup>1</sup> parameter.

In every iteration, i.e. for every time step  $\Delta t$ , one varies the value of  $m(\theta)$  at each  $\theta$ , and for each such  $m(\theta)$  variation one determines  $\delta\sigma/\delta m(\theta)$ , and then one finds the new value of  $m(\theta)$ :

$$m_{t+\Delta t}(\theta) = m_t(\theta) + \Delta t \cdot \dot{m}(\theta) \quad (4.4)$$

---

<sup>1</sup>In our experience,  $\Delta t$  is best found empirically by finding the largest value of  $\Delta t$  for which the time relaxation method still converges to a solution.  $\Delta t$  is too large when the time relaxation method does not converge to a solution.

One then reiterates until  $\sigma$  becomes acceptably small, and copies the resulting  $m(\theta)$  as the shape of mirror that would generate a desired  $I(X)$ .

Implementation of Time Relaxation method is scheduled for the second phase of this project.

## 4.4 Conclusions

We have built a successful and useful theoretical framework and a computer model for design of reflective mirrors in Uvitron's products. This accomplishment is the first milestone of Uvitron's Optical Research Program.

Our next milestone would be to implement the Time Relaxation method, for which a theoretical groundwork has been laid down in the previous section.

We are also evaluating ways to model the remaining parameters of the optical setup, such as various mirror surface coatings that are good at reflecting UV side of spectrum and absorbing other, in our case undesirable and heat producing wave-lengths.

# Bibliography

- [1] F. John Waymouth. *Electric Discharge Lamps*. The M.I.T. Press, 1988.